Assiut University Journal of Chemistry (AUJC) 47(2018) 38-50

Journal homepage: www.aujc.org

(ISSN 1678-4919) (Print) (ISSN 2357-0415) (Online)

Vol(47) No(1) 2018

Full Paper

Study of voltammetry behavior of complexation for nano-copper sulfate (NCSu) with cefdinir antibiotic (CFD) using glassy carbon electrode (GCE) in mixed 5% v/v (DMF-H_2O) solvents

E.E. El-Sherifi [1], E. A. Gomaa [2] A. A. E. Negm [2] A. M. Yousif [1]*
A. S. Abou- Elyazed[1]
[1]*Chemistry Department , Faculty of Science, Menoufia University, Shebin El-Kom, Egypt*
[2]*Chemistry Department , Faculty of Science , Mansoura University , Mansoura, Egypt.*

Email: eahgomaa65@yahoo.com

Article history : Received: 3/12/2017; Revised: 12/2/2018; Accepted : 15/3/2018; Available Online : 3/6/2018;

Abstract

Cyclic voltammetry of nano-copper (II) complex (NCSu) with Cefdinir antibiotic (CFD) was studied using a glassy carbon electrode (GCE) in 0.1M KCl as a supporting electrolyte in 5% (v/v) mixed (DMF-H_2O) solvent at two temperatures (298.15, 303.15 K). It was observed that copper (II) (NCSu) in nano form and Cefdinir antibiotic (CFD) form 1:1 and 1:2 ratio complexes. The complexation stability constants and Gibbs free energies of solvation were evaluated. Also the different thermodynamic parameters, enthalpies and entropies of complex formation were estimated. . The scan rate of nano-copper (II) (NCSu) in the absence and presence of cefdinir antibiotic (CFD) were studied. All mechanisms of electrode reactions were discussed and comparing the biological activities of bulk and nano- Cefdinir copper (II) complexes.

Keywords: Cyclic voltammetry, thermodynamics, Cefdinir antibiotic, stability constant.

1. Introduction

The unique properties of nanomaterials and structures on the nanometer scale have sparked the attention of materials developers. Over the previous decade; materials with structural features (particle size & diameter or grain size, for instance) of at least one dimension in the range 1- 100 nm, have been the subject of 100 nm, have been the subject of enormous and valuable interest [1, 2]. This is because of the high surface (HS) to the volume proportion (VP) of nanoparticles compared with macro particles (MP). Nanomaterials, that branch of materials research, are attracting a great attention because of their potential and important applications in areas such as optoelectronics (OPE) [3], catalysis [4], single-electron transistors and light emitters (LE) [5], nonlinear optical devices

(NLD) [6] photoelectrochemical (PE) [7] and biological applications. Copper (II) ions are soluble in water and play a vital role for nutrition to all higher plant and animal life. In animals, including humans, it is found widely in tissues, liver, muscle and bones. It functions as a co-factor in various enzymes and in copper based pigments [8]. Because of The accessibility of copper has it settled on it a superior decision to work with, in light of the fact that it offers properties like those of other costly respectable metals, including silver and gold. The choice of copper in the present research is attributed to have antimicrobial activity against a number of species of bacteria and fungi [9]. The complexation of medicinal substances with metal ions impact the bioavailability of drugs in the body.

The complex formation has been recommended as one of the important mechanisms for certain drug action [10]. The metal chelating phenomena re utilized to lessen the poisonous impact of drugs in human physiology [11].

Cefdiniris (6R, 7R) 7[(2 Z) 22 (2 amino1, 3 thiazole 4 y) 2(Nhydroxyimino) acetamido] -3-ethenyl-8-oxo-5-thia-1azabicyclo[4.2.0.]Oct-2-ene-2carboxylic acid is a widely used antibiotic throughout the world which is a third generation Cephalo sporin’s [12]. It is active against gram-positive and gram-negative bacteria. Bactericidal activity is because of inhibition of cell wall synthesis by acting on Penicillin Binding proteins (PBPs) [13]. The structure of Cefdinir (CED) is represented in Fig.1.

In the present research we are interested in studying the electrochemical behavior of nano-$CuSO_4$ (NCSu) at glassy carbon electrode (GCE) ,where its complexation with Cefdinir antibiotic (CFD) has been examined in 5% v/v mixed solvent (DMF-H_2O) at two temperatures (298.15, 303.15 K) and from which evaluation of the stability constant for complexation and thermodynamic parameters of the system and investigation of the broad spectrum of Cefdinir copper (II) complexes were carried out.

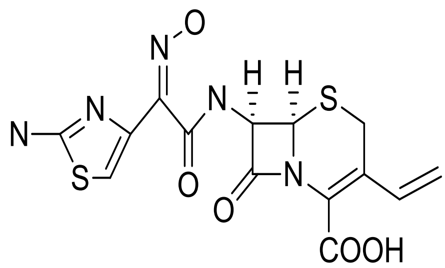

(6*R*,7*R*)-7-((*Z*)-2-(2-aminothiazol-4-yl)-2-(hydroxyimino)acetamido)-8-oxo-3-vinyl-5-thia-1-azabicyclo[4.2.0]oct-2-ene-2-carboxylic acid

Fig.1: Structural formula of Cefdinir (CED) antibiotic

2. Experimental

2.1 Materials

Cefdinir antibiotic (CED) was purchased from Sigma Aldrich and copper sulfate pentahydrate ($CuSO_4.5H_2O$) (NCSu) from Merck Germany, dimethylformamide from El Nasr pharmaceutical chemicals Co. And used directly without purification, double distilled water was used throughout this study. 5% dimethylformamide (DMF) by weight was used to insure the solubility of the used drug because small proportion of the organic solvent is enough for cyclic voltammetry.

2.2 Preparation of nano-copper sulfate (NCSu)

The nano-copper sulfate (NCSu) pentahydrate was prepared by shaking it in ball-mill apparatus of type Retsch MM2000 swing mill for period of one hour. The mill has 10 cm^3 stainless steel tubes. Two stain steel balls of 12 mm diameter were used. Ball milling was performed at 20225 Hz at room temperature and investigated under transmission electron microscopy (TEM).

Measurements

The glassy carbon electrode (GCE) was polished to a mirror like surface with 0.5 and 0.02 μm alumina in doubly distilled water. Experimental solution was deaerated by purging for at least 10 minutes with 99.99% pure nitrogen gas. Three electrodes system consists of a glassy carbon electrode (GCE) with a surface area (2.83 $x10^{-3}$ cm^2) as working electrode, Ag/AgCl (saturated with, KCl) as reference electrode and platinum wire as the counter electrode was used. Cyclic voltammetry measurement was performed using a Potentiostat Model BASi EPSILON.

3. Biological studies

3.1 Antibacterial activity

The preliminary antimicrobial activity studies of the investigated compounds was performed by the well diffusion method on different bacterial strains, Gram +ve bacteria as *Staphylococcus aureus* (*S. aureus*), Gram–ve bacteria as *Escherichia coli* (*E. coli*), ,respectively. The Nutrient agar (NA) medium was prepared by mixing peptone (5.0 g), beef extract (3.0 g), and sodium chloride (NaCl) (5.0 g) in 1,000 ml distilled water and the pH was adjusted to 6.8. A single colony inoculum (100 µl) of each bacterial strain was inoculated into 5 mL of Luria–Bertani (LB) broth and incubated for 15 hrs at shaker incubator 37°C with speed at 200 rpm and the growth was adjusted to OD 0.5. (1×10^6 CFU/ml) by using spectrophotometer (Thermo Scientific Evolution 201). Then 30 µl of the compound were dropped to a five-mm wells were made on the nutrient agar plates. Plates were incubated at 37°C for 24 h, and the clear zone was measured [14-16]. The % activity index of the compounds was determined by the following formula:

$$\%\ \text{Activity Index} = \frac{\text{Zone of inhibition by test compound diameter}}{\text{Zone of inhibition by standard diameter}}\ x\,100$$

3.2 Anti-oxidant activity screening assay using ABTS method

The antioxidant activity of the investigated compounds was assessed using 2, 2-azino-bis (3-ethylbenzothiazoline-6-sulphonic acid (ABTS) method. The radical cation derived from ABTS was prepared by the reaction of 60 mM ABTS solution with 0.3 M Manganese dioxide solution in 0.1 M phosphate buffer, pH 7. Then, the mixture was shaken, centrifuged, filtered, and the absorbance ($A_{control}$) of the resulting green-blue solution (ABTS radical solution) was measured at wave length 734 nm. Then, 50 µl of 1 mg/ml test compound in phosphate buffered methanol was added. The absorbance (A_{test}) was measured. The reduction in color intensity was expressed as % inhibition. The % inhibition for each compound is calculated from the following equation. Ascorbic acid (vitamin C) was used as standard anti-oxidant (positive control). Blank sample was run without ABTS and using MeOH/phosphate buffer (1:1) instead of sample. Negative control sample was run with MeOH/phosphate buffer (1:1) instead of tested compound [17].

$$\text{Inhibition\%} = (A_{control} - A_{testmple}) / (A_{control}) \times 100$$

3.3 Cytotoxicity assay

The human liver cancer cell lines (HepG2) were cultivated in Dulbecco’s modified Eagle’s medium DMEM supplemented with 10% (v/v) calf serum, 60 mg/mL penicillin G, and 100 mg/mL streptomycin sulfate maintained at 37 °C in a humidified atmosphere containing approximately 15% (v/v) CO_2 in air. 3-(4, 5-Dimethylthiazo l-2-yl) 2, 5-diphenyltetrazolium bromide (MTT) was used to determine the metabolic activity of cells. Living cells can reduce MTT and result in the formation of a violet product with cellular dehydrogenases. Briefly, 120-µL aliquots of the cell suspension (50,000 cells/ ml) in 96-well Microplates were incubated at 37 °C and 10% CO_2 and allowed to grow for 2 days. Subsequently, 60 µL serial dilutions of the investigated compounds were added. After 48 h of incubation, 75 µL MTT in phosphate buffered saline (PBS) was added to a final concentration of 0.5 mg mL^{-1}. After 2 h, the violet Formazan precipitate was formed. Microplates were centrifuged and the supernatant was removed. The precipitate was washed three times with 100 µL PBS and dissolved in 100 µL DMSO. The resulting color was measured at 590 nm using a plate reader (BioTek®, USA). In addition, 5-Fluorouracil was used as a positive control. All experiments were conducted as a set of two parallel experiments. The IC_{50} values were determined from the dose-response curves and it is the concentration of testing material, which showed 50% inhibition [17-19].

4. Results and Discussion

4.1 TEM image for nano-copper sulfate pentahydrate.

The pictures of the nano- $CuSO_4.5H_2O$ (NCSu) from transmission electron microscope (TEM) is represented in Figure 2 from an images we can deduce that nano- $CuSO_4.5H_2O$ (NCSu) is either in the form of irregular spheres or deformed spheres, the images show also crystalline form and the dimensions of the particles ranging from 20 to 40 nm.

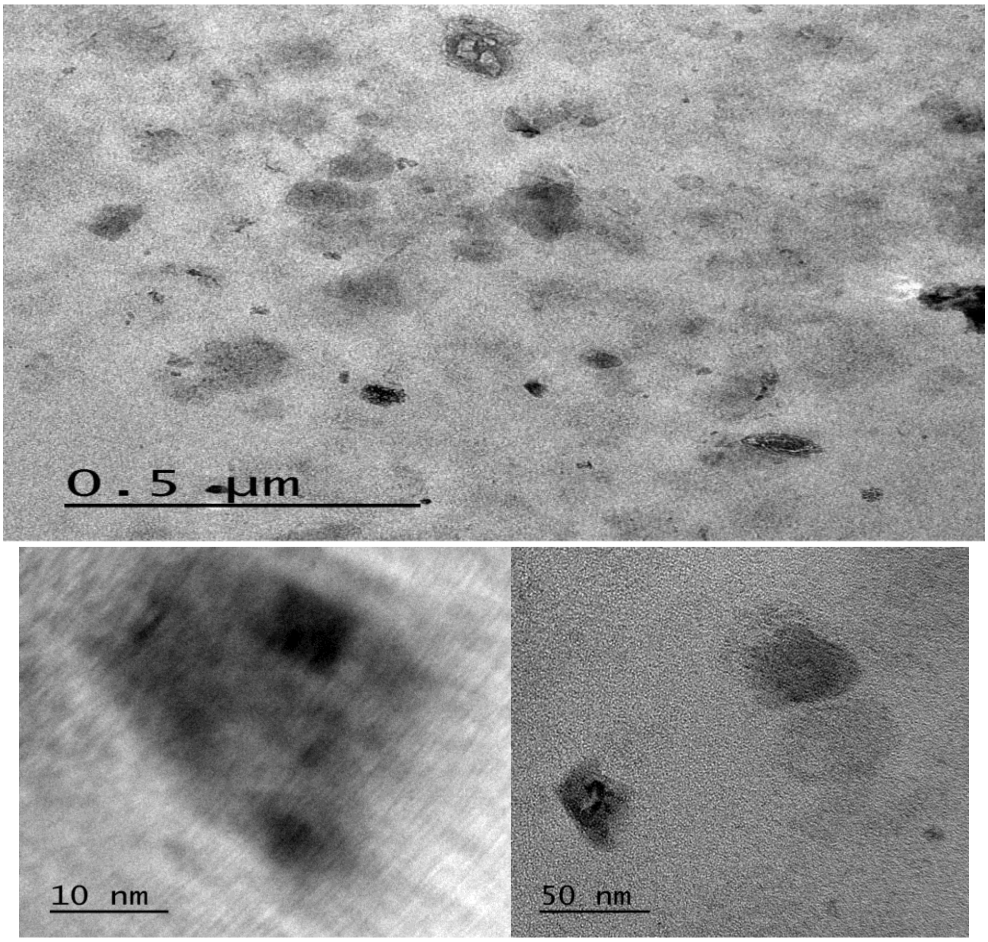

Fig. 2: TEM image of nano- $CuSO_4.5H_2O$ (NCSu)

4.2 Electrochemical behavior of nano-$CuSO_4$ (NCSu) in absence of ligand (Cefdinir drug) (CED)

The redox behavior of Cu (II) in nano- $CuSO_4$ (NCSu) was examined in 0.1 M KCl as a supporting electrolyte in 5% mixed solvent (DMF-H_2O) by cyclic voltammetry on a glassy carbon electrode (G.15 K). This process is performed at -800 to 650 mV potential window, the current is (100 µA) and 100 mV/S scan rate. In which copper sulfate solution is added in a stepwise manner to reach the final concentration CE) at different temperatures (298.15, 303 is (0.94 mM) is shown in Figure 3. From (Fig.3) it is observed that Cu^{+2} solution is electro active as it gives two anodic and two cathodic peaks (Cu^{+}/Cu^{+2}). Firstly, (at 298.15 K) for nano- $CuSO_4$ (NCSu), anodic peak current is -24.16 µA and potential -84.6 mV. Cathodic peak current is 16.45 µA and potential -387.1 mV. Secondly, (at 303.15 K) for nano- $CuSO_4$ (NCSu) anodic peak current is -25.29 µA and potential -84.6 mV. Cathodic peak current is 13.77 µA and potential -367.9 mV. This indicates that the Cu^{+2} system is a two electron reversible system.

4.3 Electrochemical behavior of nano- $CuSO_4$ (NCSu) in the presence of ligand (Cefdinir drug) (CFD)

In the present work, we are studying the complexation between cefdinir drug and nano-$CuSO_4$ (NCSu) in 5% (v/v) mixed solvent (DMF-H_2O) at two different temperatures (298.15, 303.15 K). We used two temperatures only to evaluate the thermodynamic trend for the used redox reaction , more temperatures can be used better for high precision but may give us a lot of data that makes the work big one.

In this part the drug is adding in a stepwise manner. Figure 4, represent the electrochemical behavior of complexation between nano- copper ions and Cefdinir antibiotic (CFD) in 0.1 M KCl in mixed solvent (DMF-H_2O) at (298.15, 303.15 K) at -800 mV to 650 mV potential windows, current 100 µA and scan rate 100 mV/S.

From Figure 4 It is observed that the complex is formed due to the anodic and cathodic peak decrease and potential shifts their position to lower values. Due to precipitating the complex during the process, no peak appeared. A stability constant is a measure of the strength of the interaction between the reagents that come together to form the complex. The stability constant (β_{MX}) for nano- $CuSO_4$ (NCSU) complexes in 0.1 M KCl at -800 mV to 650 mV potential windows, current 100 µA and scan rate 100 mV/S in mixed solvent (DMF-H_2O) at different temperatures (298.15, 303.15 K) for each addition were calculated [20] by applying Eq. (1).

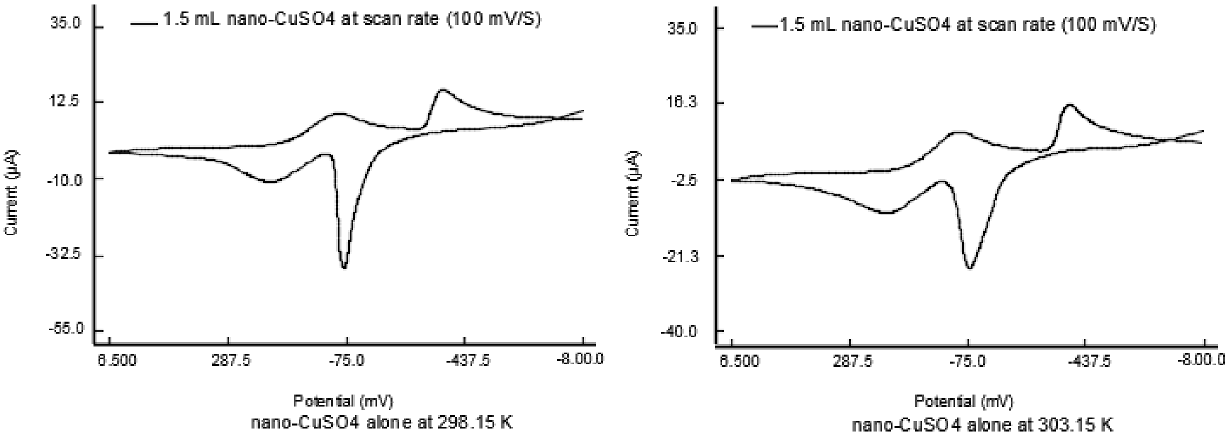

CV of nano-CuSO4 (NCSu) at 298.15 K CV of nano-CuSO4(NCSu) at 303.15 K

Fig. 3: Cyclic voltamogram of nano- $CuSO_4$ (NCSU) in 0.1M KCl at 298.15, 303.15 K.

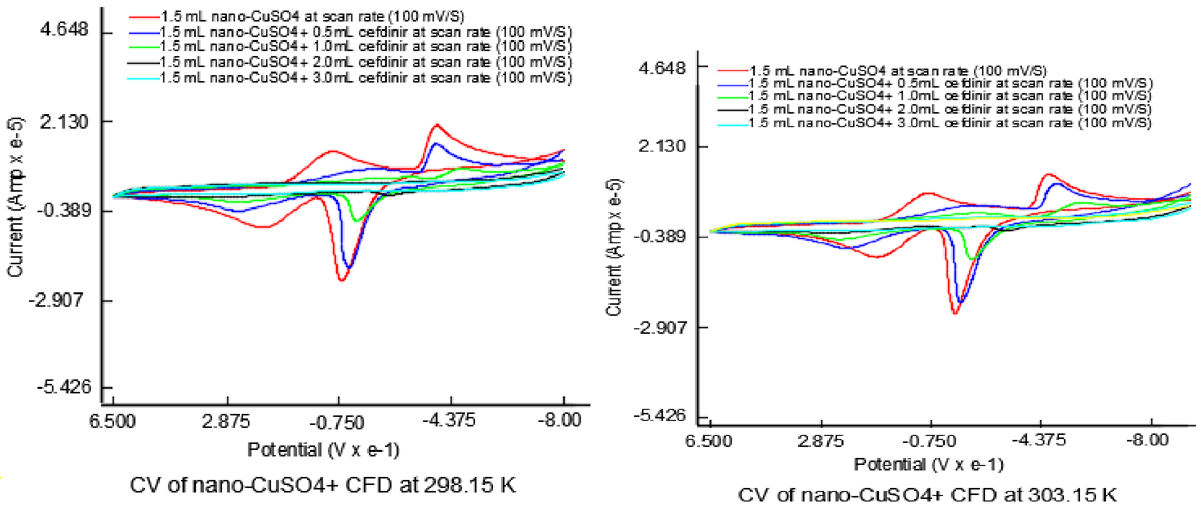

CV of nano-CuSO4 (NCSu) +CFD at 298.15 K CV of nano-CuSO4 (NCSu) +CFD at 303.15 K

Fig. 4: Cyclic voltamogram of nano- $CuSO_4$ (NCSU) in the presence of Cefdinir (CED) in 0.1 M KCl at 298.15, 303.15 K.

The Gibbs free energy of interaction for Nano-$CuSO_4$ (NCSu) with Cefdinir antibiotic (CFD) were calculated [21, 22] from stability constant (β_{MX}) using Eq (2).

All equilibrium constant vary with temperature, so the enthalpy (*ΔH*) of interaction for nano-$CuSO_4$ (NCSu) with Cefdinir antibiotic (CFD) were calculated by using Van't Hoff Eq. (3). [17-23, 24]

The entropy (ΔS) for nano- $CuSO_4$(NCSu) complexes in 0.1 M KCl at -800 mV to 650 mV potential windows, current 100 µA and scan rate 100 mV/S in mixed solvent (DMF-H_2O) at different temperatures (298.15, 303.15 K) were calculated by using Eq. (4) [25, 26].

The calculated values of ($E_{1/2}$), (β_{MX}), (ΔG), (ΔH), and (ΔS) for nano-$CuSO_4$ (NCSu) complexes in 0.1 M KCl at -800 mV to 650 mV potential windows, current 100 µA and scan rate 100 mV/S in mixed solvent (DMF-H_2O) at different temperatures (298.15, 303.15 K) were estimated in Table 1.

4.4 Mechanism of the redox reactions

The copper (II) ions used to show two oxidation peak and two reduction peaks. These two peaks corresponding to the oxidation of copper zero valent to monovalent and then the oxidation of copper monovalent to divalent cupric ions [27, 34-36].

(monovalent) then the reduction of monovalent copper to zero valent one ,copper metal involving two electrons in this media versus chloride electrode as follows :

$Cu^{+2}{}_{(aq.)} + e^- = Cu^+{}_{(aq.)}$

$Cu^+{}_{(aq.)} + e^- = Cu^o$

The vice versa for the reduction peaks is the reduction of cupric ions to cupreous silver/silver When adding Cefdinir to nano- $CuSO_4$ (NCSu) salt both peak heights were decreased indicating the reaction between them occurring and complex is formed [28, 29- 36].

4.5 Variation of the scan rate

Cyclic voltamogram of nano- $CuSO_4$ (NCSu) in absence and presence of cefdinir antibiotic in 0.1 M KCl at -800 mV to 650 mV potential windows, current 100 µA and different scan rates (50, 100, 150, 200 and 250 mV/S) at absolute temperature 298.15, 303.15 K. Represented in Figure 5,6. The peak current [30-35] for both the anodic and cathodic peaks follows Eq (5).

The plot of both anodic and cathodic peak current against the square root of scan rates (50, 100, 150, 200 and 250 mV/S) at 298.15, 303.15 K for nano- CuSO4 (NCSu) in absence and presence of cefdinir antibiotic in 0.1 M KCl at -800 mV to 650 mV potentials, current 100 µA are shown in Figures 7, 8 indicating diffusion control mechanisms [31-36] and the resulting data are listed in Tables 2, 3.

From Fig 6, its observed that as the scan rate of complex mixtures increase both corresponding peak current increase and the graph of I_p vs. $v^{1/2}$ as shown in Figures 7, 8 confirming the electrochemical processes are diffusion controlled.

$$(E_p)_M + (E_P)_C = 2.303\frac{RT}{nF}Log\beta_{MX} + 2.303\frac{RT}{nF}LogC_X \qquad (1)$$

Where $(E_p)_M$ is the peak potential of metal at final adding in absence of ligand, $(E_p)_C$ is the peak potential of metal complex, R is a gas constant (8.314 J.mol^{-1}.degree^{-1}), T is the absolute temperature and C_x is the concentration of metal in the presence of ligand.

$$\Delta G = -2.303 RT Log \beta_{MX} \quad (2)$$

$$Log \frac{\beta_2 (at T_2)}{\beta_1 (at T_1)} = \frac{\Delta H}{2.303R} \left(\frac{T_2 - T_1}{T_1 T_2} \right) \quad (3)$$

Where β_1 is the stability constant at low temperature T_1, β_2 is the stability constant at high temperature T_2.

$$\Delta G = \Delta H - T \Delta S \quad (4)$$

$$I_P = 2.69 X 10^5 n^{3/2} AC \sqrt{DV} \quad (5)$$

I_p= peak current in ampere, n = number of exchange electrons, A = area of the in mol/cm^2, V = scan rate in volts/S. electrode in cm$^{\mathbf{2}}$, D = diffusion coefficient in cm^2/s, C = concentration of the species.

Table (1): Cyclic voltammetry data of nano-$CuSO_4$ (NCSu) in the presence of Cefdinir (CED) antibiotic at 298.15, 303.15 K.

Nano- $CuSO_4$ (NCSu) in the presence of Cefdinir (CED) in 5% v/v mixed solvent (DMF-H_2O) at 298.15 K													
[M]X10^{-3}	**[L] X10^{-3}**	**[M]/[L]**	$E_{p,a}$**/mV**	$E_{p,c}$**/m**	$E_{1/2}$	$I_{p,a}$ /m**A**	$I_{p,c}$ /m**A**	β	ΔG^a	ΔH^b	$T\Delta S^c$	ΔS^d
1.89	0.303	3	-103.8	-387.1	-245.45	-21.24	11.61	2.51 x10^2	-13.69	-1.202	12.488	41.9
1.87	0.599	1.5	-132.6	-463.9	-298.25	-8.51	5.16	2.47 x10^2	-13.65	-0.609	13.041	43.7
1.85	0.857	1	-175.8	0	-87.9	-4	0	0.36 x10^2	-8.88	269.33	278.21	3.1 9
1.82	1.11	0.77	-228.6	0	-114.3	-2.14	0	0.49 x10^2	-9.649	20.072	29.721	99.7
1.8	1.35	0.6	-252.6	0	-126.5	-1.24	0	0.60 x10^2	-10.15	7.334	17.484	58.6
1.78	1.58	0.5	-382.3	0	-191.15	-0.83	0	0.83 x10^2	-10.96	-40.49	-29.53	99.04
Nano- $CuSO_4$ (NCSu) in the presence of Cefdinir (CED) in 5% v/v mixed solvent (DMF-H_2O) at 303.15 K													
[M]X10^{-3}	**[L] X10^{-3}**	**[M]/[L]**	$E_{p,a}$**/mV**	$E_{p,c}$**/m**	$E_{1/2}$	$I_{p,a}$ /m**A**	$I_{p,c}$ /m**A**	β	ΔG^a	ΔH^b	$T\Delta S^c$	ΔS^d
0.91	0.303	3	-108.6	-391.9	337	-22.33	11.24	2.49 x10^2	-13.91	-1.202	12.708	41.9
0.88	0.599	1.5	-137.4	-463.9	310	-10.06	5.93	2.46 x10^2	-13.88	-0.609	13.271	43.8
0.86	0.857	1	-190.2	-555.1	286.5	-3.77	3.89	2.16 x10^2	-13.55	269.33	88 282	-933.1
0.84	1.11	0.77	-233.4	0	257	-2.14	0	0.56 x10^2	-10.15	20.072	30.222	-99.7
0.81	1.35	0.6	-252.6	0	248.5	-1.68	0	0.63 x10^2	-10.44	7.334	17.774	58.6
0.79	1.58	0.5	-271.9	0	86	-0.98	0	0.63 x10^2	-10.46	-40.49	-30.03	-99.1

^{a} **ΔG (kJ/mol), ^{b} ΔH (kJ/mol), ^{c} $T\Delta S$ (kJ/mol), ^{d} ΔS (J/mol.K).**

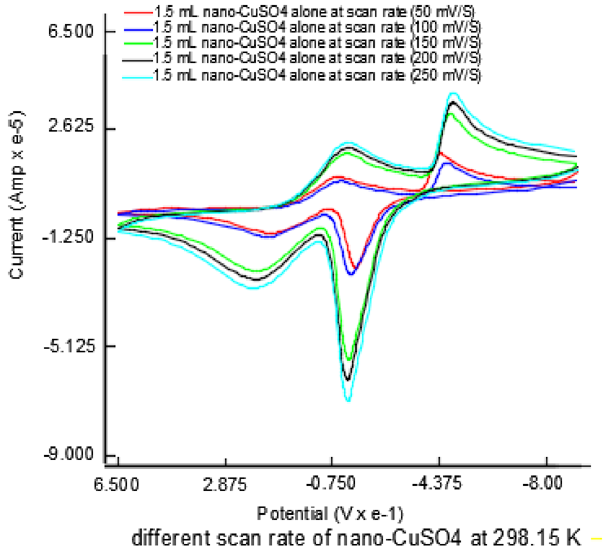

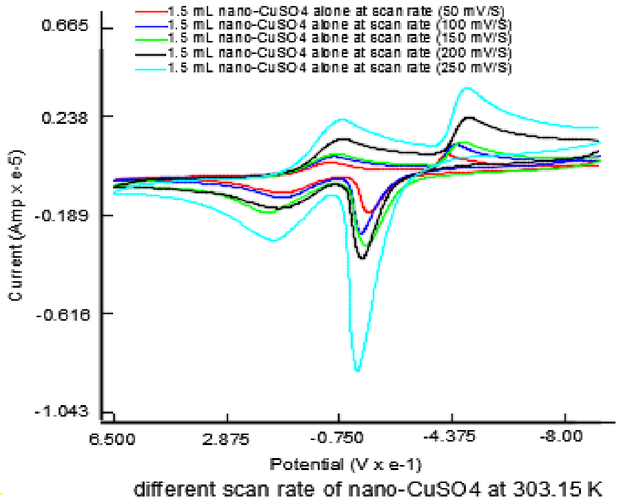

CV of scan rates nano-$CuSO_4$ (NCSu) at 298.15 K CV of scan rates nano-$CuSO_4$ (NCSu) at 303.15 K

Fig. 5 Cyclic voltamogram of nano- $CuSO_4$ (NCSu) in absence of Cefdinir (CED) antibiotic in 0.1 M KCl at 298.15, 303.15 K and different scan rates (50, 100, 150, 200 and 250 mV/S).

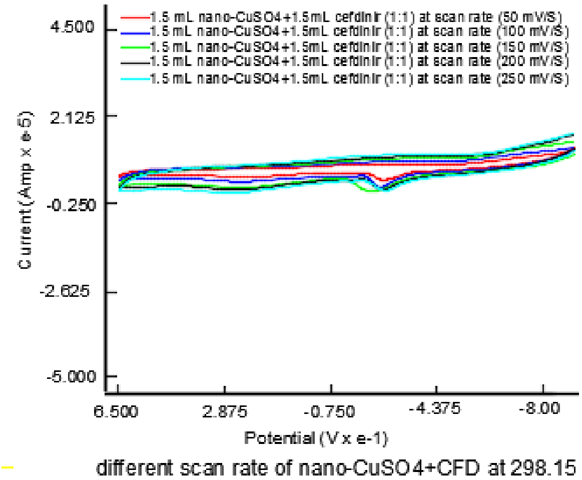

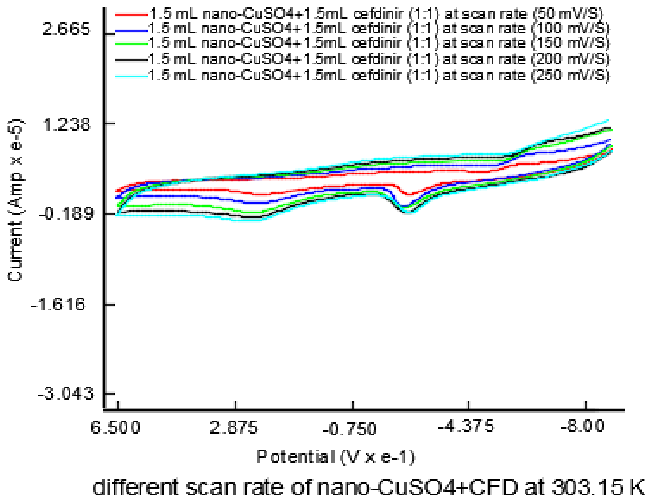

CV of scan rates nano-$CuSO_4$ (NCSu)+CFD at 298.15 K CV of scan rates nano-$CuSO_4$(NCSu) +CFD at 303.15 K

Fig. 6: Cyclic voltamogram of nano-$CuSO_4$ (NCSu) in the presence of Cefdinir (CED) antibiotic (1:1) in 0.1 M KCl at 298.15, 303.15 K and different scan rates (50, 100, 150, 200 and 250 mV/S).

Table 2: Cyclic voltammetry data of nano- $CuSO_4$ (NCSu) in absence of Cefdinir (CED) antibiotic in 0.1 M KCl at 298.15, 303.15 K and different scan rates (50, 100, 150, 200 and 250 mV/S).

			Nano-CuSO4 ((NCSu) at 298.15 K				Nano-CuSO4 (NCSu) at 303.15 K			
[M] x10-3	V	v 1/2	**Ip,a /µA**	**Ip,c /µA**	**Da/cm2.s-1**	**Dc/cm2.s-1**	**Ip,a /µA**	**Ip,c /µA**	**Da/cm2.s-1**	**Dc/cm2.s-1**
0.94	0.05	0.224	-21.84	19.93	1.09 X 10-11	9.09 X 10-12	-15.83	9.23	3.91 X 10-12	1.33 X 10-12
0.94	0.1	0.316	-24.16	16.45	1.04 X 10-11	4.83 X 10-12	-25.29	13.77	8.46 X 10-12	2.51 X 10-12
0.94	0.15	0.387	-55.67	34.54	4.34 X 10-11	1.67 X 10-10	-30.21	14.75	9.31 X 10-12	2.22 X 10-12
0.94	0.2	0.447	-63.3	39	4.99.X 10-11	1.89 X 10-11	-36.45	26.45	1.39 X 10-11	7.34 X 10-12
0.94	0.25	0.5	-70.67	42.22	4.19 X 10-11	1.49 X 10-10	-87.21	39.83	6.38 X 10-11	1.33 X 10-11

All diffusion parameters are greater at 298.15 than 303.15K for interaction of nano $CuSO_4$ (NCSu) with Cefdinir CED) antibiotic in 5% v/v mixed DMF-H_2O solvents.

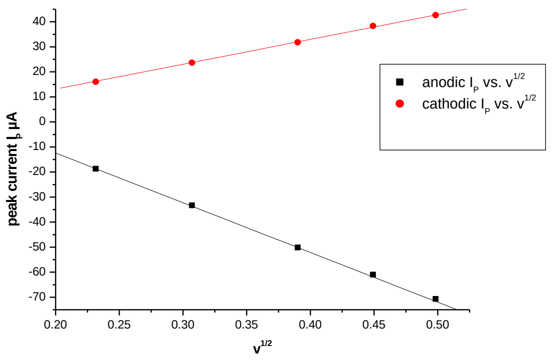

Peak current Ip vs. $V^{1/2}$ for nano-$CuSO_4$(NCSu) at 298.15 K

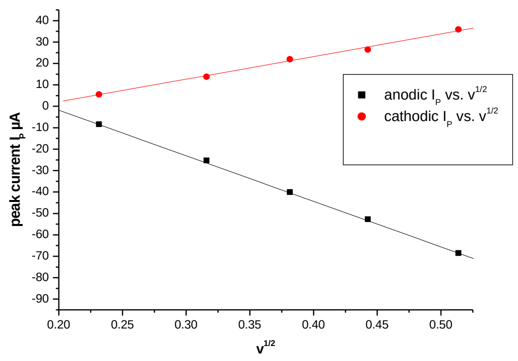

Peak current Ip vs. $V^{1/2}$ for Nano-$CuSO_4$(NCSu) at 303.15 K

Fig. 7: The plot of both anodic and cathodic peak current against the square root of scan rate at 298.15, 303.15 K for nano- $CuSO_4$ (NCSu) in absence of Cefdinir (CED) antibiotic.

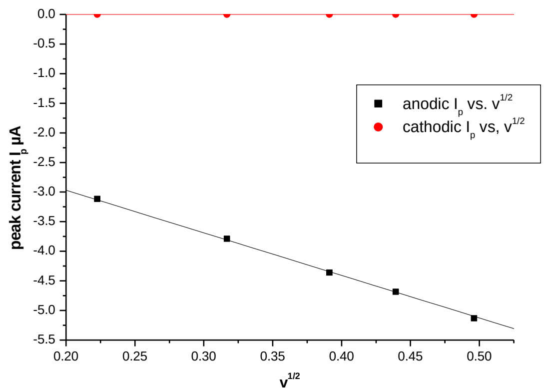

Ip vs. $V^{1/2}$ for nano(NCSu)-$CuSO_4$ + CFD (1:1) at 298.15 K

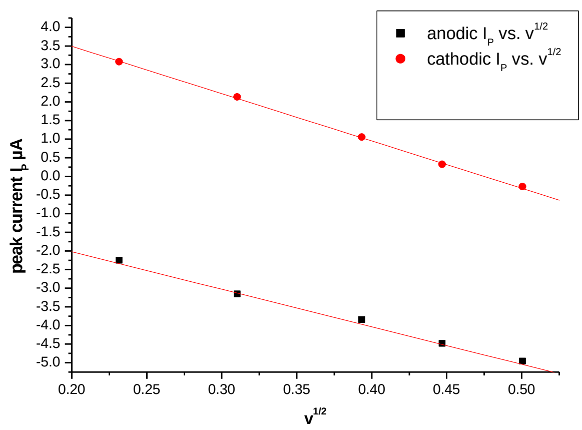

Ip vs. $V^{1/2}$ for nano(NCSu)-$CuSO_4$ + CFD (1:1) at 303.15 K

Fig. 8: The plots of both anodic and cathodic peak current against the square root of scan rate at 298.15, 303.15 K for nano-$CuSO_4$ (NCSu) in the presence of Cefdinir antibiotic (CFD).

Table 3: Cyclic voltammetry data of nano-$CuSO_4$ (NCSU) in the presence of cefdinir (CED) antibiotic (1:1) in 0.1 M KCl at 298.15, 303.15 K and different scan rates (50, 100, 150, 200 and 250 mV/S).

			Nano-$CuSO_4$(NCSu) + CFD at 298.15 K (1:1)				Nano-$CuSO_4$(NCSu) + CFD at 303.15 K (1:1)			
[M] $x10^{-3}$	V	$V^{1/2}$	**$I_{p,a}$ /μA**	**$I_{p,c}$ /μA**	**$D_a/cm^2.s^{-1}$**	**$D_c/cm^2.s^{-1}$**	**$I_{p,a}$ /μA**	**$I_{p,c}$ /μA**	**$D_a/cm^2.s^{-1}$**	**$D_c/cm^2.s^{-1}$**
0.86	0.05	0.224	-2.61	0	7.34×10^{-14}	0	-2.06	2.48	1.80×10^{-13}	2.61×10^{-11}
0.86	0.1	0.316	-4.23	0	6.66×10^{-14}	0	-3.54	3.89	4.47×10^{-13}	5.40×10^{-13}
0.86	0.15	0.387	-5.16	0	4.38×10^{-14}	0	-3.77	0	5.13×10^{-14}	0
0.86	0.2	0.447	-4.23	0	4.84×10^{-14}	0	-4.64	0	5.83×10^{-14}	0
0.86	0.25	0.5	-4.9	0	5.19×10^{-14}	0	-4.9	0	5.75×10^{-14}	0

5. Biological studies of Cefdinir drug and Cu^{+2} complex

5.1 Antibacterial activity of Cefdinir and Cu^{+2} complexes

To analyze the antibacterial activity against gram-positive and gram-negative bacteria, the agar well diffusion test was used. Ampicillin was used as a standard antibiotic for gram-positive and gram-negative bacteria. The diameter of the inhibition zone around each well and the activity index (AI) was determined and compared to the standard antibiotics (Table 4). The estimated mean inhibition zone and activity index against gram-negative bacteria of Cefdinir was higher than Cu^{+2} nano complex and Cu^{+2} bulk complex more than three fold. On the other hand, the mean inhibition zone and activity index against gram- positive bacteria of Cefdinir were approximately similar to Cu^{+2}bulk complex and higher than Cu^{+2} nano complex more than six fold. Therefore, it can be concluded that Cu^{+2}bulk complex shows a higher antibacterial activity against gram-positive bacteria than that against gram-negative bacteria. Furthermore, the antibacterial activity of Cefdinir against both bacteria was significantly reduced upon complexation with Cu^{+2} nano complex.

There are several assays for evaluating the antioxidant properties of compounds; however, the *in vitro* ABTS assay is commonly used to investigate the radical scavenging activities of compounds. The antioxidant activity of a compound is estimated by its ability to scavenge the $ABTS^{\cdot}$ by the decrease in the absorbance. As depicted in Table 5, Cefdinir, Cu^{+2} nano complex and Cu^{+2} bulk complex showed a moderate antioxidant activity.

5.2 Cytotoxic activity of Cefdinir and Cu^{+2} complexes against MCF-7 and HepG2 cell lines

To confirm if the investigated compounds are potentially interesting candidates for cancer therapy, we initially aimed to verify if the newly synthesized compounds possessed any cytotoxic activity. Therefore, cytotoxicity assays were conducted against the human cancer cell lines MCF-7 and HepG2, which are suitable models for drug targeting. Cytotoxicity was calculated from the dose-response curves and is expressed as the compound concentration that reduces the absorbance of the treated cells by 50% (IC_{50}). Table 3 showed that Cefdinir and its bulk Cu^{+2} complexes were able to strongly reduce the viability of MCF-7 cell lines. Notably, phenotypic changes, including cell morphology and cell–cell adhesion were also observed in the culture after the treatment However, Cu^{+2} nano and bulk complexes reduce the viability of HepG2with moderate IC_{50}.

Table 4 : The estimated mean inhibition zone and activity index of Cefdinir and its bulk and nano Cu^{+2} complexes

	E. coli		***S. aureus***	
Compound	**Diameter of inhibition zone (mm)**	**% Activity index**	**Diameter of inhibition zone (mm)**	**% Activity index**
Cefdinir	11	45.8	17	77.3
Cu+2nano complex	2	8.3	3	13.6
Cu+2bulk complex	3	12.5	14	63.6
Ampicillin	24	100	22	100

Table 5 : Antioxidant activity.

Compounds	Absorbance of samples	% inhibition
Control of ABTS	**0.510**	**0%**
Ascorbic-acid	**0.058**	**88.6%**
Cefdinir	**0.322**	**36.9%**
Cu^{+2}nano complex	**0.382**	**25.1%**
Cu^{+2} bulk complex	**0.318**	**37.6%**

Table 6: Cytotoxic activities of Cefdinir and its bulk and nano Cu^{+2} complexes on the viability of HepG2 and MCF-7 cell lines

Compounds	In vitro Cytotoxicity IC50 (μg/ml)	
	HepG2	MCF-7
5-Fluorouracil	**7.9±0.17**	**5.4±0.20**
Ligand	**10.3±0.94**	**9.7±0.72**
Cu^{+2}nano complex	**54.2±2.98**	**72.3±4.11**
Cu^{+2} bulk complex	**37.1±2.13**	**16.2±1.34**

Conclusion

The overall stability constants (β) and Gibbs free energies of complex formation ΔG for interaction of nano $CuSO_4$ (NCSu) with Cefdinir (CED) antibiotic are slightly greater at 298.15K than that at 303.15K in 5% v/v Mixed DMF-H_2O solvents indicating more interaction and complexation .The enthalpies and entropies for the interaction of nano $CuSO_4$ (NCSu) + Cefdinir antibiotic (CED) are almost the same in the used two temperatures. This indicates the increase of temperature is followed by decrease of complexation ability in this mixed solvents due to the migration of ions away from complexation field by increase of temperature as cyclic voltammetry explained. We found cefdinir copper (bulk) complex exhibited higher biological activity as antibacterial, antifungal and anti- oxidant than Cefdinir and Cefdinir copper (nano) complex. Generally, this means upon complexation with bulk copper ions resulted in lowering the toxicity of the ligands.

References

1. V. Mody Vicky, Siwale Rodney ,Singh Ajay and R.Mody Hardik, J.Pharm.Bioallied Sci., 2 (2010) 282.

2. O.Salata, J. Nanobiotechnol , 2 (2004)1

3.P. Ko-Ying and DA-Hua Wei, Nanaomaterials, 6 (2016) 140.

4. T. Franklin , Metal nanoparticles for catalysis : Advances and application, Royal Society of Chemistry,Thomas House,Science Park , Milton Road , Cambridge, UK (2014).

5.K.I. Bogutska ,Yu.P..Sklyarov ,Yu I.Prylutskyy, Ukraninica Biorganica Acta, 1 (2013) 9.

6. S. Suresh and D. Arivuoli, Res. Adv. Mater.Sci.,30 (2012) 243.

7. M Christa and I. Grozescu , Chem.Bull . Politechnica Univ. (Timisoura),54 (2009) 1.

8. M.Ali ,F. Zhou K. Chen , C. Kotzur , C. Xiao, L. Bourgeois, X. Zhang,D. R. Farlane, Nature Communications, 7(2016)1.

9. S. Magdassi, M. Grouchko and Alexander K., Materials , (2010) 4626..

10.A.K. Chatterjee , R.Chakraborty ,T. Basu., Nanotechnology, 4, 25 (2014) 135101 .

11. W. Lin, I.Stayton ,Y Huang, Z. Dong, and Y. Ma, , Toxicological & Environmental Chemistry, 90, 5-6(2008) 983.

12. R. Platt, Journal of Antimicrobial Chemotherapy,10(1982) 135.

13. O. Gutten and L. Rulisek, Inorg . Chem.,52(18)(2013)10347.

14. B Mounyr ,Si Moulay,K. Ibn Souda Saad, A review, Journal of Pharmaceutical Analysis. 6 (2016)71–79.

15. S. Shaik, M. Kummara, S. Poluru, C. Allu, J. Gooty, C. Rao Kashayi, and M. Subha; International Journal of Carbohydrate Chemistry Volume (2013)1.

16. B Holt.Katherine and A. J. Bard, Biochemistry, 44 (2005) 13214.

17.E. Lissi ,B. Modak ,R. Torres ,J. Escobar ,A Urzua ,Free Rad.Res.,30(1999)471.

18. H.J. Mauceri, N.N. Hanna, M.A. Beckett D.H. Gorski, M.J. Staba, K.A.Stellato, K. Bigelow,R. Heimann, S. Gately, M. Dhanabal, G.A. Soff, V.P. Sukhatme, D.W. Kufe, R,R. Weichselbaum, Nature, 394(6690), (1998) 287.

19. H. M.Killa, J. Chem. Soc.Faraday Trans. I, 81(1985) 2659.

20. B.E.Conway , Ann Rev Phys Chem.; 17(1966) 481 .

21. A.A. El-Khouly ,E.A. Gomaa and S.M.Abou El-leef S., Bull Electrochem.; 19(4) (2003) 153 .

22. A.A. El-Khouly ,E.A. Gomaa and S.M. Abou El-leef S., Bull. Electrochem. , 19(5)(2003)193.

23. E.A.Gomaa , Int J Mater Chem. , 2(2012)16.

24. E.A.Gomaa andB.M. Al-Jahdali., Am. J Fluid Dynamics. 1(2011) 4 .

25.E.A. Gomaa ,. Analele Universitate din Bucuresti Chimie, 19(2010) 45 .

26.P.K Casey.,J.C. Christopher, and G.T. Donald, J Phys Chem-B. 110(2006) 16066 .

27.Esam A. Gomaa , Physics. Chem. Liq. 50(2012) 279.

28.Esam A. Gomaa, Int J Mater Chem. 2 (2012)16 .

29. Esam A.Gomaa , Am. J Polymer Sci. , 2(3) (2012) 35 .

30.Esam A. Gomaa , Eur Chem Bull. 1 (2013) 259.

31. Esam A.Gomaa ,Elsayed M. Abou Elleef , E.A.Mahmoud, Eur Chem Bull.2 (2013)732.

32.E. A. Gomaa, E Abou Elleef , Am. Chem Sci J., 3(2013) 489.

33. E. A.Gomaa ,A.E.Negm ,R. M.Abu Qarn , American Association for Science and Technology, AASCIT Communi-cations , 3,3 (2016)177 .

34. E. A.Gomaa ,E. M Abou Elleef , Sci . Technol. 3(2013)118 .

35.Esam A. Gomaa ,Rania R. Zaky , Amr E. Negm , Radwa T. Rashad , American Association for Science and Technology, AASCIT Communications, 3,5(2016) 224.

36. Esam A. Gomaa , Amr E.Negm , A.Tahoon , European Journal of Chemistry,7(2016) 341 .